The Effect of Supercritical Carbon Dioxide on Polymer-Solvent Mixtures

Anastassios A. Kiamos and Marc D. Donohue*

Department of Chemical Engineering, The Johns Hopkins University, Baltimore, Maryland 21218

Received February 26, 1993; Revised Manuscript Received July 22, 1993•

ABSTRACT: The high-pressure phase behavior of polymer-solvent-supercritical carbon dioxide systems was investigated experimentally. The polymers used were poly(methyl methacrylate), polystyrene, polybutadiene, and poly(vinyl ethyl ether) at concentrations ranging from 5 to 10% in mixtures with toluene or tetrahydrofuran. The experiments were conducted for temperatures from 25 to 70 °C and pressures up to 2200 psia in a high-pressure cell. The effect of the nature of the solvent on the L-LL phase transition was determined. Specifically, interest is focused on the effect of the supercritical carbon dioxide concentration on the mixture phase boundaries.

Introduction

Applications of supercritical fluids have received considerable attention during the past 20 years, and, for a variety of reasons, interest in these fluids is likely to grow. Because of their unusual properties they can be used in a wide range of processes such as fractionation of polymers, extraction of monomers from high molecular weight oils and polymers, purification of reactive monomers, and precipitation of polymers from solution by supercritical antisolvents. Other applications operated at supercritical conditions include gas absorption and polymerization. A number of commercial processes involve a combination of two or more of the above. In industry, supercritical fluids also are used for specialized operations which include separation of drugs from plants, caffeine from coffee, oils from vegetable seeds, impurities from labile materials, and chemical feedstocks from coal and petroleum residue.[1]

Recently, a new "clean" technology for spraying paints has been developed which reduces emissions of volatile organic compounds (VOC) that cause ozone depletion, simply by replacing the VOC with supercritical carbon dioxide, an environmentally compatible gas.[2] This new process has the potential for reducing emissions of VOC's from the spraying of paints by up to 80%.[3] To reformulate paints and other coatings so they can be sprayed by this process will require knowledge of the high-pressure phase behavior of polymer-solvent-supercritical fluid mixtures. Unfortunately, there are few data in the literature on these systems, particularly for the range of concentrations being used in commercial applications.

We present here the result of a systematic series of experiments that help to explain the thermodynamic behavior of polymer-solvent-supercritical fluid mixtures. To our knowledge, there are no previously published data for the range of concentrations of polymer and solvent studied here.

Phase Behavior

Understanding the phase behavior of high-pressure mixtures is important to the design of supercritical fluid processes. Unfortunately, accurately modeling the phase equilibia of high-pressure systems, especially for polymer mixtures, is problematic as there are a number of theoretical questions that have not yet been answered adequately to allow quantitative calculations. In cases where the molecular weight distribution of the polymer is very narrow, with the polydispersity resonably close to unity, the mixture can be considered pseudobinary.[4] However, when the polymer is polydisperse the phase behavior can become extremely complex.

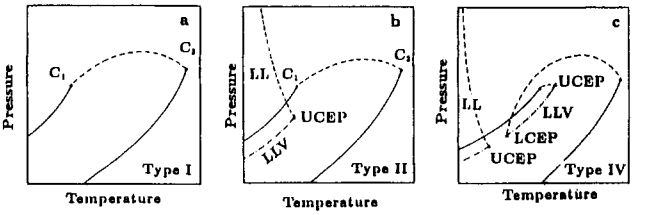

Figure 1. Three of the six types of phase behavior diagrams described by Van Konynenburg and Scott.[5]

Van Konynenburg and Scott were the first to systematically classify the phase diagrams of binary mixtures.[5] They used the van der Waals equation of state and identified six fundamental types of binary systems, three of which are shown in Figure 1. Recently, two new phase diagrams have been identified.[6] Boshkov[7] performed calculations using the Ree equation of state and optimized some of the equation parameters to find a seventh type of phase behavior. Gallagher et al.[8] used computer simulations to calculate an eight type of phase behavior which is expected to exist in CF_4/NH_3 mixtures.

Type I equilibria (Figure 1, plate a) are found in binary mixtures that are close to ideal solution behavior.[9] The pure-component vapor-liquid equilibrium boundary lines terminate at the pure-component critical points, C_1 and C_2. In the case of binary hydrocarbon mixtures, the critical point of the heavier hydrocarbon (C_2) is located at a pressure lower than that of the lighter component. The vapor-liquid critical mixture curve, shown as a dashed line, runs continuously from C_1 to C_2, and it may be monotonic or show either a maximum or minimum. An example of Type I behavior is found in $CO_2/n\text{-}C_4H_{10}$ mixtures.

As the two components in the mixture become more dissimilar, e.g., CO_2/C_8H_{18} mixtures, Type II equilibria (Figure 1, plate b) are observed. The vapor-liquid critical locus remains a continuous line, but there is an area of liquid-liquid immiscibility at low temperatures. The upper critical solution temperature (UCST) is a function of pressure as shown. There also is a three-phase liquid-liquid-vapor equilibrium region where the L-L equilibrium surface interests the V-L equilibrium surface. The

* To whom correspondence should be addressed.
• Abstract published in *Advance ACS Abstracts*, December 15, 1993.

0024-9297/94/2227-0357$04.50/0

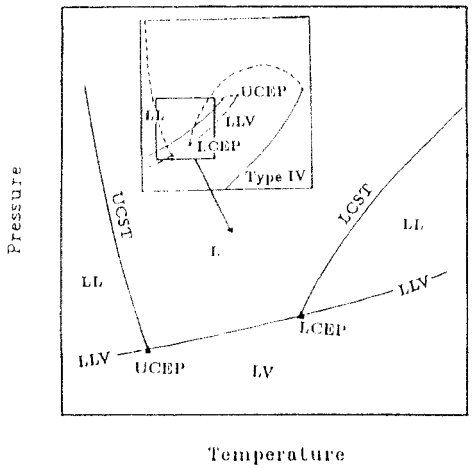

Figure 2. Region of pressure–temperature space on the phase diagram where the experiments in this work were conducted.

three-phase region ends at the upper critical end point (UCEP).[10]

The type of phase behavior observed in this work is shown in plate c of Figure 1 and is classified as Type IV behavior. As in Type II, there is a region of limited liquid miscibility at low temperatures, ending at an UCEP. However, in Type IV systems, a second region of limited miscibility appears from the LCEP (lower critical end point) to a second UCEP at higher pressures and temperatures. A characteristic of this type of phase behavior is that the vapor–liquid critical mixture curve is not continuous but has two branches.

Figure 2 shows schematically the domain in P–T space where the experiments in this study have been conducted. As the molecular weight of a polymer increases, the vapor pressure of the polymer becomes close to zero, and the LLV equilibrium line in P–T space projects on the L–LV boundry of the solvent. The boundary separating the single liquid phase region from the second region of limited liquid miscibility at high temperatures is referred to as the lower critical solution temperature (LCST) line. The LCST line intersects the vapor–liquid equilibrium boundary of the solvent at the LCEP. There also are three-phase regions separating both LL regions and the LV region. However, for the types of systems studied here, the three-phase regions are narrow and therefore for simplicity are shown as LLV lines.

The addition of carbon dioxide into a binary polymer–solvent mixture changes the system to ternary and hence changes the system's behavior. The phase boundaries move as the concentration of carbon dioxide is increased in the system. The LCST line moves to lower temperatures and higher pressures, the UCST line moves to higher pressures and temperatures, and the L–LV boundary moves to higher pressures. Figure 3 shows schematically the effect of supercritical fluid addition to the mixture. The rate that the LCST and UCST lines shift to higher pressures is greater than the shift of the L–LV boundary line. At high carbon dioxide concentrations, the LCST and UCST curves merge, resulting in a phase behavior that has no L–LV boundary.

Figure 4 shows schematically the phase behavior of a ternary mixture when the pressure and the temperature remain the same and the compositions of the three components change. This type of triangular phase diagram only exists at combinations of temperature and pressure for which a LLV region is formed. For low polymer concentrations, adding a supercritical fluid moves the mixture from the single-phase region (point 1) into the

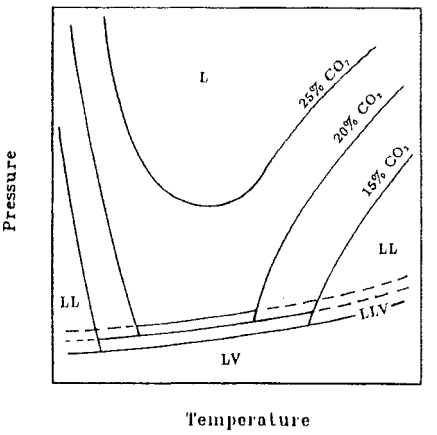

Figure 3. Schematic representation of the effect of supercritical fluid concentration increase in a polymer–solvent–supercritical fluid mixture.

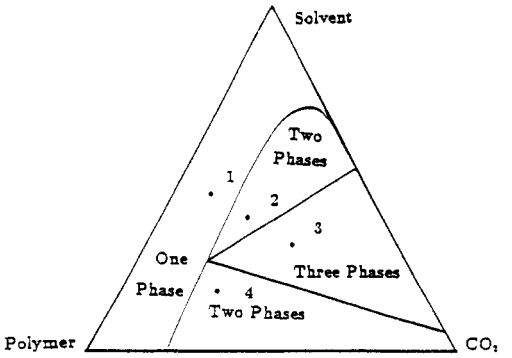

Figure 4. A schematic polymer–solvent–CO_2 ternary diagram. Addition of carbon dioxide (at constant T and P) can cause the system to go from one phase to two phases and then to three phases.

liquid–liquid region (point 2). Further increase of the SCF brings the system into the three-phase region (liquid–liquid–vapor or liquid–liquid–fluid) (point 3). In such mixtures the vapor phase typically contains more than 90% CO_2 and very little polymer. For medium to high polymer concentrations, the addition of CO_2 brings the system into a liquid–vapor area (point 4).

Experiments

The experiments reported in this work were performed in a Phaser III supercritical phase analysis unit. This apparatus was designed specifically for the analysis of the phase behavior of supercritical CO_2/polymeric resin mixtures. The apparatus is based on experimental designs by McHugh and co-workers[11] and was made by Union Carbide Corp. The information which may be obtained using the Phaser includes densities, viscosities, solubilities, and P–T phase boundaries. A description and a schematic diagram of the apparatus and the experimental procedure, as well as the technique for determining the phase boundaries are described in detail elsewhere.[12,13] Several modifications have been made to the apparatus to improve its operation. First, the pressure generators are not manual but are driven by electric motors. There also is a counter on the drive mechanism that allows calibration of the volume of hydraulic fluid that has been pumped into the cell. Second, the cell is not held in an air bath but has ten heating elements embedded in it. This allows the cell to equilibrate faster to new temperature settings, and hence the experiments are more efficient. Finally, the measurement of the amount of CO_2 added to the cell has been made more accurate. The CO_2 holding tank that feeds the cell with supercritical fluid is set on an electronic balance with ±0.1-g accuracy. The amount of the CO_2 introduced into the cell can be determined from the difference of the balance readings before and after loading. The pressure in the feed lines and the holding cell is the same before and after the feeding procedure, since saturated liquid CO_2 is used.

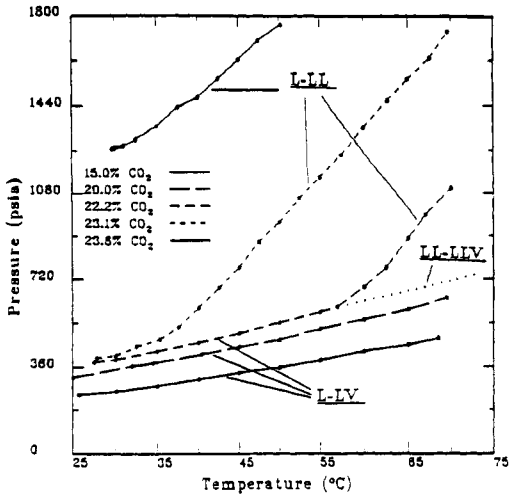

Figure 5. Polystyrene/tetrahydrofuran/carbon dioxide phase diagram for mixtures with a 4/1 tetrahydrofuran/polystyrene ratio.

The data points obtained from the experiments are best represented on a pressure–temperature diagram. Figure 5 shows a typical *P–T* diagram for a mixture of 4/1 THF/polystyrene for various CO_2 compositions. Each line of data points is for a constant concentration of carbon dioxide. The data points represent two different kinds of phase transitions, i.e., liquid to liquid–vapor and the liquid to liquid–liquid phase transitions. The transition from the single liquid phase to the liquid–vapor region is a line with a small slope and appears at low CO_2 concentrations. As the CO_2 concentration increases, there is a change in slope of this line. The point where the change in slope occurs moves to lower temperatures as the CO_2 concentration increases. The data on the steeper line represent the boundary between the single liquid phase and the liquid–liquid region. The extrapolation of the L–LV line to higher temperatures shows where the three–phase region must exist.

It should be noted that the phase diagrams presented here have all the characteristics of the critical point curves calculated by Van Konynenburg and Scott. However, the experimental results presented here are not mixture critical curves. They are merely phase diagrams. In fact, in most cases, the data presented here are quite far from the mixture critical lines because of the mixture compositions studied. Therefore, the phase boundaries of the phase diagrams presented here are not referred to as LCST and LCST lines but as L–LL phase boundaries. [We apologize for the awkwardness of this terminology, but it is necessary to avoid confusion concerning the nature of the phase diagrams.]

Materials

Solvents. The toluene (reagent grade) was obtained from Baker. The THF (99+% ACS reagent, catalog no. C10,030-7) was obtained from Aldrich Chemical Co., Inc.

Polymers. Poly(methyl methacrylate), average MW 120 000 (catalog no. 18,233-0), was obtained from Aldrich Chemical Co., Inc.

Polybutadiene (36% cis, 55% trans-1,4, 9% vinyl), average MW 420 000 (catalog no. 052); polybutadiene (20% vinyl, 80% cis and trans-1,4), average MW 5000 (catalog no. 894); polystyrene, average MW 235 000 (catalog no. 846); and poly(vinyl ethyl ether), average MW 3800 (catalog 154) were obtained from Scientific Polymer Products, Inc.

Supercritical Fluid. For all experiments the supercritical fluid used was carbon dioxide (99.8% minimum purity), bone dry, supplied by Matheson Gas Products, Inc.

Results and Discussion

Table 1 lists the concentrations of polymer, solvent, and carbon dioxide studied in this work. The experimental data points are shown in the following figures and are tabulated elsewhere.[12] A total of 24 systems were studied[12] with THF or toluene as a solvent, but for the sake of brevity not all of them are discussed here. The phase behaviors of various polymers when THF is used as a solvent are shown in Figures 6–8. The systems shown in these figures are representative of systems with different solvent/polymer ratios (on a CO_2-free basis). In Figures 9–11 are general results that come from this study and the comparison of the above systems.

Figure 6 shows a *P–T* diagram for mixtures of THF/poly(methylmethacrylate) at solvent/polymer ratios of 5.7/1, 4/1, and 3/1. The polymer solution in Figure 6 has a THF/PMMA ratio of 3/1 and is studied for CO_2 concentrations of 15.0, 20.0, 25.0, 27.1, and 29.1%. [The carbon dioxide concentrations are reported as weight percent of total.] For low CO_2 concentrations, 15.0 and 20.0% CO_2, only the L–LV boundary was seen for the temperature range studied. For 25.0% CO_2, at 50.0 °C the liquid to liquid–liquid (L–LL) boundary appears, with the characteristic change of the slope. For 27.1% CO_2 the L–LL boundary moves to lower temperatures, and for 29.1% CO_2 it moves further to lower temperatures and higher pressures, so that no data for the L–LV boundary were seen in the *P–T* range of the apparatus. Therefore, as the supercritical fluid concentration increases, the L–LV boundary shifts to higher pressures and the (LCST-like) L–LL boundary shifts to lower temperatures and higher pressures. The rate that the L–LL boundary moves to lower temperatures is about 7 °C for every 1% increase in the CO_2 concentration. The slope of the L–LL boundary remains approximately constant and is 43 psi/°C.

Figure 7 shows a *P–T* diagram for THF–polystyrene mixtures for a solvent/polymer ratio of 4/1 and CO_2 concentrations of 15.0, 20.0, 21.0, 22.2, 23.1, and 23.6%. For CO_2 concentrations up to 21.0%, only the L–LV boundary has been observed. For 22.2% CO_2 and at 57.0 °C, the L–LL boundary appears, with the characteristic change of slope. As the supercritical fluid concentration increases, the L–LL boundary shifts to lower temperatures and higher pressures. The slope of the L–LL boundary for 22.2% CO_2 is approximately 44 psi/°C. For 23.1% CO_2 the slope becomes 39 psi/°C, and for 23.6% CO_2 the slope is 27 psi/°C. It is obvious that the increase of the CO_2 in the system changes the slope and the boundary is becoming more horizontal. This is an indication that the L–LL boundaries from the two liquid–liquid envelopes will merge to a curve that shows a minimum with further increase of SCF.

Figure 8 shows a *P–T* diagram for THF with polybutadiene. The mixture in Figure 8 has a ratio of 19/1 THF/PB and is studied in concentrations of 20.0, 25.0, 30.0, 35.0, and 40.0% CO_2. For concentrations up to 35% CO_2 only the L–LV boundary was observed. For 40% CO_2 the mixture was in the two liquid phase region for the entire operating range, and so no data for the two-phase boundary were obtained. The L–LV boundaries have similar slopes, but there is a tendency for the slopes to increase as the SCF ratio increases. For example, for 20% CO_2 the slope is 4.7 psi/°C and becomes 6.9, 8.5, and finally 8.9 psi/°C for 35% CO_2. Another interesting observation concerns how the distance between the L–LV boundary changes. The rate of the shift to higher pressures decreases as the SCF concentration increases. For example, at 60 °C the distance between the 20 and 25% vapor pressure line is 144.3 psi, then it drops to 91.3 psi between 25 and 30%, and it further drops to 73.3 psi between 30 and 35%.

A comparison of mixtures of a solvent (THF in this case) with different polymers shows interesting results for the L–LV and the L–LL boundaries. Comparing the

Table 1

polymer	THF/polymer	wt % CO_2	polymer	THF/polymer	wt % CO_2
poly(methyl methacrylate), av MW 120 000	5.7/1	15.0	polystyrene, av MW 235 000		15.0
		20.0			20.0
		25.0		3/1	21.6
		30.0			23.1
		32.3			24.0
		33.7			15.0
		20.0		2/1	20.0
		25.0			23.8
	4/1	30.0	polybutadiene, av MW 420 000	19/1	20.0
		31.7			25.0
		33.0			30.0
		15.0			35.0
		20.0			25.0
	3/1	25.0		9/1	30.0
		27.1			35.0
		29.1			25.0
polystyrene, av MW 235 000	5.7/1	20.0		5.7/1	30.0
		25.0			35.0
		26.0			
		15.0			
		20.0			
	4/1	21.0			
		22.2			
		23.1			
		23.6			

polymer	toluene/polymer	wt % CO_2	polymer	toluene/polymer	wt % CO_2
poly(methyl methacrylate), av MW 120 000	5.7/1	15.0	polystyrene, av MW 235 000		17.5
		20.0		1.9/1	20.0
		25.0			22.5
		30.0			24.3
		35.8	polybutadiene, av MW 5000	9/1	15.0
		37.4			20.0
		39.9			25.0
		41.3			30.0
		20.0			35.0
		25.0			40.0
		30.0			15.0
	4/1	33.3		2/3	20.0
		34.9			25.0
		36.3			26.6
		38.5			15.0
		20.0		1/3	20.0
	2/1	24.2			22.0
		30.0		1/9	15.0
		31.3	poly(vinyl ethyl ether), av MW 3800	1/4	15.0
polystyrene, av MW 235 000	5.7/1	15.0			20.0
		20.0			25.0
		25.0			30.0
		27.6			35.0
		20.0			40.0
		25.0			15.0
	4/1	25.9			20.0
		27.3		1/9	25.0
		28.1			30.0
		15.0			35.0
		20.0			40.0
	3/1	25.0			15.0
		26.1			20.0
		26.9		pure PVEE	25.0
	2/1	14.6			30.0
		25.0			37.6

above diagrams, it can be seen that the L–LV equilibrium is sensitive to SCF concentration and shifts to higher pressures as the concentration of the CO_2 increases. The rate of shift to higher pressures decreases as the CO_2 ratio increases, as illustrated in Figure 8.

However, the L–LV boundary is not sensitive to the polymer or its concentration (for low to medium polymer concentrations). In Figure 9, five systems are compared on the same P–T diagram, with 19/1, 9/1, and 5.7/1 THF/PB, 5.7/1 THF/PS, and 5.7/1 THF/PMMA. The concentration of CO_2 in all of these systems was 25%. The L–LV boundaries for all the systems have almost the same slope, and many of the data points overlap. At lower pressures, or lower CO_2 concentrations, the L–LV boundaries of the systems also are a group of lines with very little difference in slope.

The boundary between the single liquid and the two liquid phase area is very sensitive to SCF concentration. All of the diagrams for these mixtures show how rapidly this phase boundary moves to higher pressures as the concentration of the SCF increases. The changes of the SCF concentration also can cause differences in the slope and even differences in the shape of the boundary, especially when it forms a curve that shows a minimum.

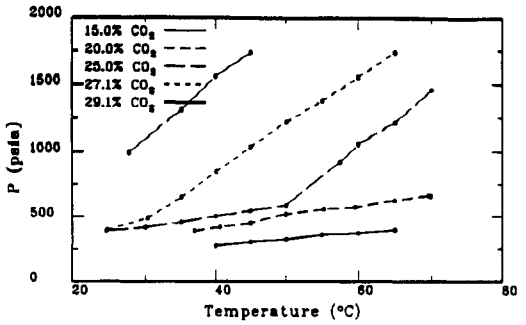

Figure 6. Poly(methyl methacrylate)/tetrahydrofuran/carbon dioxide phase diagram for mixtures with a 3/1 tetrahydrofuran/poly(methyl methacrylate) ratio.

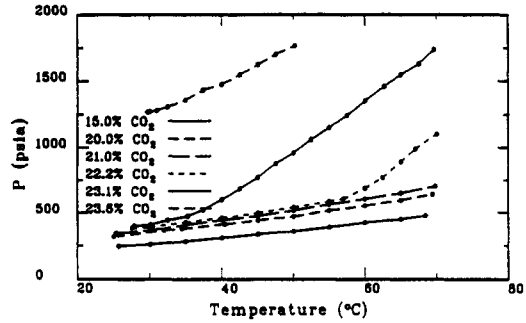

Figure 7. Polystyrene/tetrahydrofuran/carbon dioxide phase diagram for mixtures with a 4/1 tetrahydrofuran/polystyrene ratio.

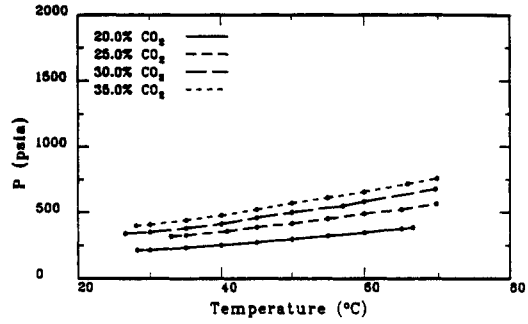

Figure 8. Polybutadiene/tetrahydrofuran/carbon dioxide phase diagram for mixtures with a 19/1 tetrahydrofuran/polybutadiene ratio.

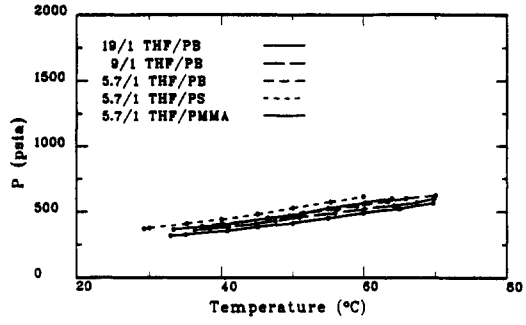

Figure 9. *P–T* projection of the L–LV boundary curves for systems with polybutadiene, polystyrene, and poly(methyl methacrylate) in tetrahydrofuran with 25.0% w/w carbon dioxide.

The L–LL boundary also depends on the polymer concentration. Figure 10 shows the L–LL boundary for systems with 5.7/1, 4/1, and 3/1 THF/PS in mixtures with 23.1% CO_2. The L–LL boundary for 4/1 THF/PS has been shifted to lower temperatures and higher pressures compared to the one with 5.7/1 THF/PS. But the L–LL boundary for 3/1 THF/PS is at higher temperatures and lower pressures than the curve for 4/1 THF/PS, even though the polymer concentration is higher. The explanation for this phenomenon comes from understanding the phase behavior in three dimensions. The L–LL boundary is a projection of the two liquid boundary surface on a *P–T* plane. The shape of this surface is a dome, and variation of the *P–T* projection with polymer concentration depends on which side of the dome the system is on. There are cases where all the data are on the same side of the dome, and so the L–LL boundary seems to move to lower temperatures continuously. For the system studied here, the 5.7/1 and 4/1 THF/PS L–LL boundaries are located on the one side of the dome, and the 3/1 THF/PS L–LL boundary is located on the other side of the dome. Hence it moves back to higher temperatures as the polymer concentration is increased.

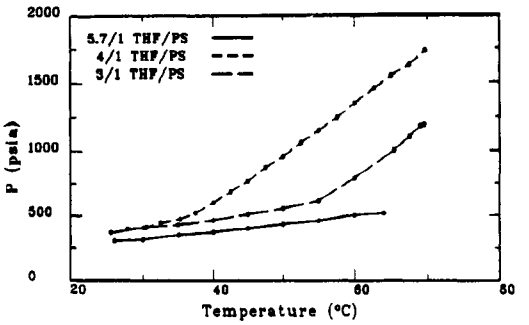

Figure 10. Comparison of the L–LL boundary curve for systems with 23.1% carbon dioxide, the same solvent and polymer, but different solvent to polymer ratio.

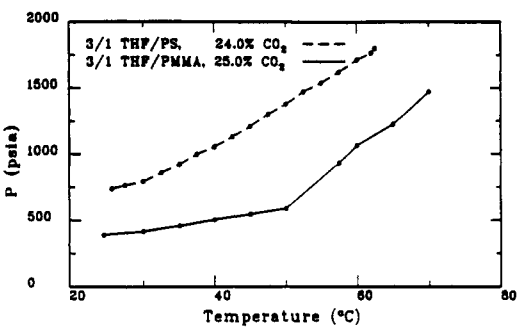

Figure 11. Comparison of the L–LL boundaries for systems with similar carbon dioxide concentration for poly(methyl methacrylate) and polystyrene in tetrahydrofuran.

The liquid to liquid–liquid boundary depends on the nature on the polymer. The importance of the polymer structure can be seen by studying systems with similar CO_2 composition and the same solvent. Figure 11 shows the experimental data points for the L–LL equilibria for systems of 3/1 THF/polymer (PMMA or PS). The L–LL boundary for the PS system has been taken for 24.0% CO_2, and the 25.0% CO_2 line is expected to be at slightly higher pressures and lower temperatures. From the figure it is seen that the L–LL boundary for the PMMA is located at much lower pressures and higher temperatures than the one for PS.

The phase behaviors of various polymers when toluene is used as a solvent are shown in Figures 12–15. As before, for the sake of brevity, the systems shown in these figures are representative of a group of experiments where toluene was used as a solvent. Figures 16 and 17 show cross-plots of the information in Figures 12–15.

Figure 12 shows a *P–T* diagram for experiments with PMMA–toluene mixtures in a solvent/polymer ratio of 4/1. The polymer solution is studied for concentrations of CO_2 of 20.0, 25.0, 30.0, 31.6, 33.3, 36.3, and 38.5%. For 20.0 and 25.0% CO_2, only the L–LV boundary was observed. From 30.0 to 36.3% CO_2 VLE and LLE were

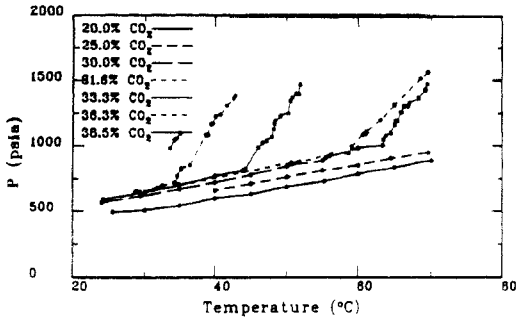

Figure 12. Poly(methyl methacrylate)/toluene/carbon dioxide phase diagram for mixtures with a 4/1 toluene/poly(methyl methacrylate) ratio.

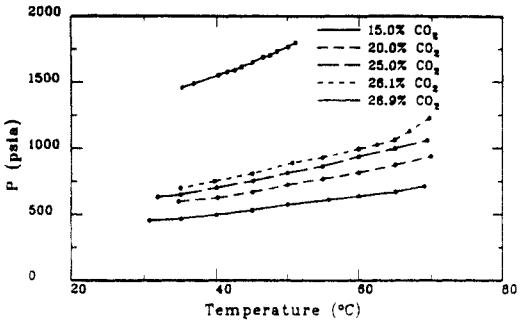

Figure 13. Polystyrene/toluene/carbon dioxide phase diagram for mixtures with a 3/1 toluene/polystyrene ratio.

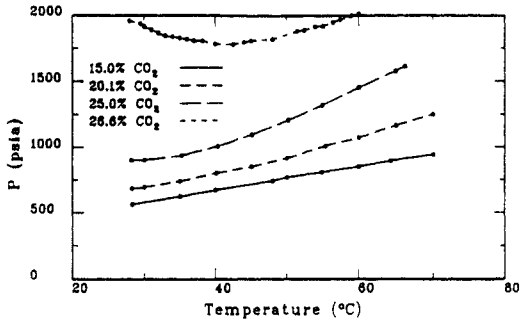

Figure 14. Polybutadiene/toluene/carbon dioxide phase diagram for mixtures with a 2/3 toluene/polybutadiene ratio.

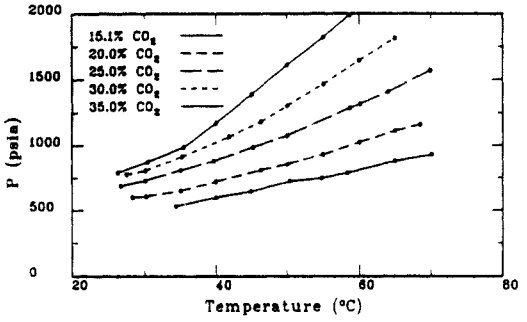

Figure 15. Poly(vinyl ethyl ether)/toluene/carbon dioxide phase diagram for mixtures with a 1/9 toluene/poly(vinyl ethyl ether) ratio.

seen. One should note how rapidly the L–LL boundary moves to lower temperatures and higher pressures as the SCF ratio increases, whereas the L–LV boundary is almost constant. For 38.5% CO_2 only the LLE is observed. The slope of the L–LL boundary remains approximately the same at 77 psi/°C.

Figure 13 shows one *P–T* diagram from a group of experiments with ratios of 5.7/1, 4/1, 3/1, and 1.9/1 of toluene with polystyrene.[12] The polymer solution in this figure has a ratio of 3/1 toluene/PS and is studied for

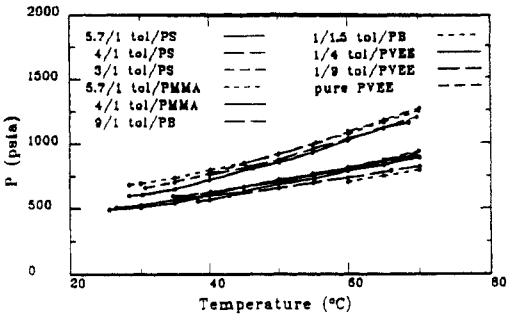

Figure 16. *P–T* diagram for polybutadiene, polystyrene, poly(methyl methacrylate), and poly(vinyl ethyl ether) in toluene for 20.0% carbon dioxide.

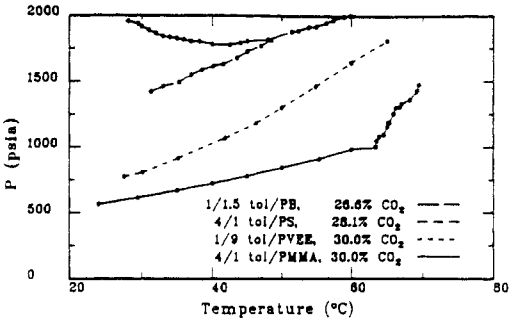

Figure 17. Comparison of the L–LL boundaries for systems with the same solvent, similar amounts of carbon dioxide, but different polymer concentrations.

concentrations of CO_2 of 15.0, 20.0, 25.0, 26.1, and 26.9%. For CO_2 concentrations up to 25.0% CO_2, only the L–LV boundary, was observed within the operating temperature range. For 26.1% CO_2 and at 65.0 °C the L–LL boundary appears. It is very sensitive to the SCF concentration as an increase of CO_2 concentration by 0.8% shifts the boundary about 45 °C lower in temperatures or 800 psi higher in pressure.

Figure 14 shows one *P–T* diagram from a group of experiments with polybutadiene–toluene mixtures with solvent/polymer ratios of 9/1, 2/3, 1/3, and 1/9. The polymer solution in this figure has a ratio of 2/3 toluene/PB and is studied for concentrations of CO_2 of 15.0, 20.1, 25.0, and 26.6%. For 15.0% CO_2 concentrations, only the L–LV boundary has been observed. For 20.1 and 25.0% CO_2, the boundaries do not show the sudden change of the slope as in the previous systems. Some of the data are at pressures higher than the critical pressure of CO_2 (about 1070 psi). The fact that the abrupt change of the slope does not occur in these systems is believed to be due to the low molecular weight of the polymer. At 26.6% CO_2 the boundary between the single liquid phase and the two liquid phase region shows a minimum. The L–LL boundary has this shape because it merges with the second LL envelope that appears at lower temperatures. Under these conditions there is no path from the single liquid phase to the vapor–liquid region that does not pass through the two-liquid region.

Figure 15 shows one *P–T* diagram from a group of experiments with poly(vinyl ethyl ether)–toluene mixtures with solvent/polymer ratios of 1/4 and 1/9 and pure polymer. The polymer solution in this figure has a toluene/PVEE ratio of 1/9 and is studied for concentrations of CO_2 of 15.0, 20.0, 25.0, 30.0, and 35.0%. As in the previous system, since the molecular weight of the polymer is low, the L–LV boundary and the L–LL boundary are smooth, without any sudden change in slope. Also in this case, the slope increases from 11 psi/°C for 15% CO_2 to 15.4, 21.1, 28.8, and finally 42.4 psi/°C for 35.0% CO_2.

The comparison of systems with different polymers, polymer concentrations, and CO_2 concentrations gives important information about the VLE and the LLE. Similar to the THF case, the L–LV boundary is sensitive to SCF concentration, and the boundary shifts to higher pressures as the concentration of CO_2 increases. On the other hand, the VLE is not very sensitive to the different polymers and different polymer concentrations for low to medium polymer concentrations, but there are differences as the polymer concentration increases to more than a 1/1.5 solvent/polymer ratio.

In Figure 16, 10 systems are compared on the same diagram. The CO_2 concentration is 20% in all of the systems. Systems with ratios of 5.7/1, 4/1, and 3/1 toluene/PB, 5.7 and 4/1 toluene/PMMA, and 9/1 toluene/PB belong to the group of systems with low to medium polymer concentration, and they all fall within a small range of pressures. The L–LV boundaries for all the systems have the same slope and many of the data points are overlapping. Systems with ratios of 1/1.5 toluene/PB, 1/4 and 1/9 toluene/PVEE, and pure PVEE belong to the group with high polymer concentration. This group of lines is located at higher pressures and the slopes of the boundaries are larger. The deviation of these boundaries from the previous group is due to the different solvent activity as the volume fraction of polymer in the system exceeds about one-third.

The boundary between the single liquid and the two liquid phase region is very sensitive to SCF concentration and moves to lower temperatures and higher pressures as the concentration of the SCF increases. The increase of the SCF concentration can cause differences in the slope and differences in the shape of the boundary. The L–LL boundary also is strongly dependent on the polymer and its concentration.

Figure 17 shows a comparison of systems with different polymers and approximately the same amount of CO_2. At very high pressures the L–LL boundary for 26.6% CO_2 in a mixture with a ratio of 1/1.5 toluene/PB is observed. The PB–toluene systems show limited miscibility even for low amounts of CO_2 in the mixture. The boundary shows a minimum at 43.0 °C. Studying the system's behavior, the 30% CO_2 L–LL boundary is expected to be at least 500 psi higher. Below this, the L–LL boundary for 28.1% CO_2 in a solution with a ratio of 4/1 toluene/PS appears. For this system also, the 30% CO_2 boundary is expected to be at higher pressures and lower temperatures. The next lines are for 1/9 toluene/PVEE and 4/1 toluene/PMMA, both with 30% CO_2. For the PMMA system, the L–LL boundary appears at temperatures higher than 65 °C. Of these systems, the PMMA–toluene system at 30% CO_2 shows the largest area of miscibility.

The discussion above has dealt with the effects of the supercritical fluid and the polymer concentration on the phase behavior of the mixture. In Figures 18 and 19, the effect of the solvent on the VLE and the LLE is shown. In these figures, data points for systems with the same polymer and the same amount of supercritical fluid are compared.

In Figure 18, six systems with the same CO_2 concentration (20.0%) and the same polymer (PS) are compared when toluene and THF are used as solvents. The L–LV boundaries of these systems appear in two groups, approximately with the same slope but with different pressures. The group of the L–LV boundaries at higher pressures belong to systems where toluene is the solvent. Even for different amounts of polymer, the boundary remains at the same pressure. The group of the lines that

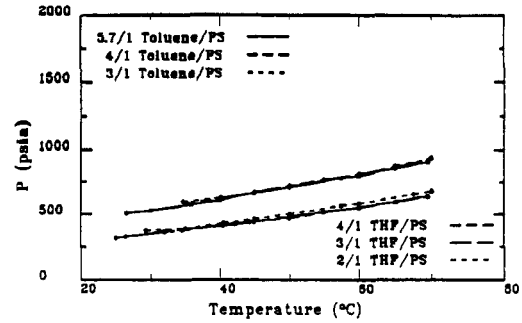

Figure 18. L–LV boundary curves for 20% carbon dioxide in polystyrene systems when toluene and tetrahydrofuran are used as solvents.

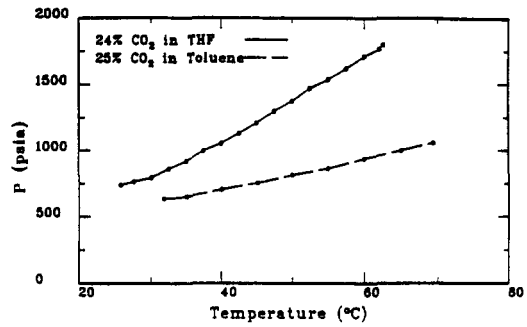

Figure 19. L–LL boundary curves for 25% carbon dioxide in polystyrene systems when toluene and tetrahydrofuran are used as solvents.

appear at lower pressures are for systems where THF was used as a solvent. Therefore, CO_2 dissolves better in THF, and the L–LV boundary for the THF systems is at lower pressures than for the toluene systems.

The dependence of the LLE on the solvent is shown in Figure 19. In the figure, two systems with a 3/1 ratio of sovlent to PS are compared for toluene and THF as the solvents. The difference between the two systems is obvious. The L–LL boundary for THF is at much lower temperatures and higher pressures than for toluene. It should be mentioned that the system with THF has only 24% CO_2, and the 25% CO_2 line is expected to be at even higher pressures than the line that is shown in the figure. With THF as a solvent and PS as a polymer, we observed L–LV boundaries at lower temperatures and lower pressures, compared to the toluene systems, but L–LL boundaries at higher pressures and lower temperatures, compared to the toluene systems. So the CO_2 is entrained better in THF than in toluene, but it moves the LLE to much lower temperatures and higher pressure and hence THF increases the immiscibility area more than toluene.

Conclusions

A systematic investigation of polymer–solvent–supercritical fluid mixture phase behavior was made. Supercritical carbon dioxide acts as an antisolvent for these systems. This behavior is due to the large difference between the gas-like density of the supercritical fluid and the liquid-like density of the solvent–polymer binary. Addition of supercritical carbon dioxide decreases the area of miscibility by shifting the L–LL boundary to lower temperatures and higher pressures and the L–LV boundary to higher pressures. The L–LV equilibrium does not depend on the nature or the concentration of the polymer but does depend on the solvent. Mixtures with THF show L–LV boundaries at much lower pressures compared to mixtures where toluene is used as the solvent.

The L–LL equilibrium is very sensitive to the supercritical fluid concentration. The concentration of the polymer, the polymer nature, and the solvent nature can also affect the equilibrium. For several systems examined in this work, the L–LL boundary at higher temperatures (LCST-like) merges with the L–LL boundary at lower temperatures (UCST-like), resulting in a curve that goes through a minimum in pressure when plotted versus the temperature.

Acknowledgment. The authors wish to acknowledge support of this research by the National Science Foundation and Union Carbide Corp. Financial support of this research by the Chemical and Thermal Systems Division of the NSF (Contact No. CTS-9216923) was provided under their program for Environmentally Benign Chemical Processing. We also are grateful to Dr. Kenneth Nielsen, Dr. John Argyropoulos, and Mr. Richard Bailey of Union Carbide Corp. for technical support of the research reported here.

Abbreviations

C_1	critical point for the more volatile component
C_2	critical point for the heavy component
LCEP	lower critical end point
LCST	lower critical solution temperature
LL	liquid–liquid
L-LLE	liquid to liquid–liquid equilibrium
LLV	liquid–liquid–vapor
PB	polybutadiene
PMMA	poly(methyl methacrylate)
PS	polystyrene
PVEE	poly(vinyl ethyl ether)
SCF	supercritical fluid
THF	tetrahydrofuran
UCEP	upper critical end point
UCST	upper critical solution temperature
VLE	vapor–liquid equilibrium
VOC	volatile organic compound

References and Notes

(1) McHugh, M. A.; Krukonis, V. J. Processing Polymers and Monomers with Supercritical Fluids. *Encycl. Polym. Sci. Eng.* **1989**, *16*, 368.
(2) Lee, Chinsoo; Hoy, Kenneth L.; Donohue, Marc D. Supercritical Fluids as Diluents in Liquid Spray Application of Coatings. *U.S. Patent* 4,923,720, May 8, 1990.
(3) Nielsen, K. A.; Glancy, C. W.; Hoy, K. L.; Perry, K. M. A New Atomization Mechanism for Airless Spraying: The Supercritical Fluid Spray Process. *Fifth International Conference on Liquid Atomization and Spray Systems*, Gaithersburg, MD, July 15–18, 1991.
(4) Seckner, A. J.; McCellan, A. K.; McHugh, M. A. High-Pressure Solution Behavior of the Polystyrene–Toluene–Ethane System. *AIChE J.* **1988**, *34*, 9.
(5) Van Konynenburg, P. H.; Scott, R. L. *Philos. Trans. R. Soc. London, Ser. A* **1980**, *298*, 495–540.
(6) Van Pelt, A.; Peters, C. J.; de Swaan Arons, J. Liquid–liquid immiscibility loops predicted with the simplified-perturbed-hard-chain theory. *J. Chem. Phys.* **1991**, *95* (10), 15.
(7) Boshkov, L. Z. *Dokl. Akad. Nauk SSSR* **1987**, *294*, 901.
(8) Gallagher, J. S.; Peters, C. J.; Levelt Sengers, J. M. H., private communications.
(9) Ekart, M. P.; Brennecke, J. F.; Eckert, C. A. Molecular Analysis of Phase Equilibria in Supercritical Fluids. *Supercritical Fluid Technology: Reviews in Modern Theory and Applications*; CRC Press, Inc.: Boca Raton, 1991; pp 163–192.
(10) Prausnitz, J. M.; Lichtenthaler, R. N.; de Azevedo, E. G. *Molecular Thermodynamics of Fluid-Phase Equilibria*; Prentice-Hall: Englewood Cliffs, NJ, 1986.
(11) McHugh, M. A.; Guckes, T. L. Separating Polymer Solutions with Supercritical Fluids. *Macromolecules* **1985**, *18*, 674.
(12) Kiamos, A. A. High Pressure Behavior of Polymer–Solvent–Supercritical Fluid Mixtures. M.S. Thesis, The Johns Hopkins University, 1992.
(13) Seckner, A. J. Experimental Studies of Supercritical Fluid Phase Behavior. M.S. Thesis, The Johns Hopkins University, 1987.